

Effects of Vanadium doping on BaFe_2As_2

XING-GUANG LI^{1 (a)}, JIE-MING SHENG^{1,2 (a)}, CONG-KUAN TIAN¹, YI-YAN WANG¹, TIAN-LONG XIA¹, LE WANG¹, FENG YE², WEI TIAN², JIN-CHEN WANG¹, JUAN-JUAN LIU¹, HONG-XIA ZHANG¹, WEI BAO¹ and PENG CHENG^{1 (b)}

¹ *Department of Physics and Beijing Key Laboratory of Opto-electronic Functional Materials & Micro-nano Devices, Renmin University, Beijing 100872, China*

² *Neutron Scattering Division, Oak Ridge National Laboratory, Oak Ridge, TN 37831, USA*

PACS 74.70.Xa – Pnictides and chalcogenides

PACS 74.62.Dh – Effects of crystal defects, doping and substitution

Abstract – We report an investigation of the structural, magnetic and electronic properties of $\text{Ba}(\text{Fe}_{1-x}\text{V}_x)_2\text{As}_2$ using x-ray, transport, magnetic susceptibility and neutron scattering measurements. The vanadium substitutions in Fe sites are possible up to $\sim 40\%$. Hall effect measurements indicate strong hole-doping effect through V doping, while no superconductivity is observed in all samples down to 2 K. The antiferromagnetic and structural transition temperature of BaFe_2As_2 is gradually suppressed to finite temperature then vanishes at $x=0.245$ with the emergence of spin glass behavior, suggesting an avoided quantum critical point (QCP). Our results demonstrate that the avoided QCP and spin glass state which were previously reported in the superconducting phase of Co/Ni-doped BaFe_2As_2 can also be realized in non-superconducting $\text{Ba}(\text{Fe}_{1-x}\text{V}_x)_2\text{As}_2$.

Introduction. – In both cuprate and Fe-based high- T_c superconductors, investigation of the interplay between the magnetism and superconductivity through chemical doping is critical to explore the superconducting mechanism [1, 2]. In the iron-pnictides phase diagram, besides superconductivity and antiferromagnetic (AFM) phase, various exotic states including incommensurate short-range AFM order, G-type AFM order, C_4 magnetic phase and spin glass state were observed which reveals the rich physics controlled by the interplay between the spin, charge and orbital degrees of freedom in this system [3–11].

For the well-known FeAs-122 parent compound BaFe_2As_2 , either electron doping (e.g., Co, Ni, Cu, Rh, Ir, Pt, Pd) [12–15] or isoelectronic doping (e.g., Ru, P) [16, 17] in the FeAs plane could easily instigate superconductivity. On the hole doping side, although alkali metal doping in the Ba site could induce superconductivity with transition temperature as high as 38 K [18], attempts of hole doping in the FeAs plane (e.g., Mn, Cr, Mo) [5, 7, 19] show that the stripe AFM and structural transitions are suppressed to some extent but superconductivity was never observed. This contrasting behavior has not been well understood. Furthermore, the discovery of a novel C_4 magnetic phase

only in the hole-doped 122 materials has drawn a lot of research interests [9]. Therefore more investigations are needed for the hole doping cases in the FeAs plane.

In this paper we report the effect of V-doping on BaFe_2As_2 in a bulk property and neutron/x-ray diffraction study. The hall effect measurements indicate that V substitution for Fe results in hole doping. Although superconductivity is not observed in $\text{Ba}(\text{Fe}_{1-x}\text{V}_x)_2\text{As}_2$ as in other in-plane hole-doping cases, an avoided Quantum critical point with the emergence of spin glass state are found in heavily doped samples.

Experiment. – Single crystals of $\text{Ba}(\text{Fe}_{1-x}\text{V}_x)_2\text{As}_2$ were grown by FeAs/VAs self-flux method similar to $\text{Ba}(\text{Fe}_{1-x}\text{Co}_x)_2\text{As}_2$ [20]. Polycrystalline samples were synthesized by heating stoichiometric Barium, FeAs and VAs in an evacuated quartz tube at 1223 K for 30 h. The products were reground and annealed at the same temperature twice to ensure the phase purity. The elemental doping composition was measured by energy dispersive x-ray spectroscopy (EDS, Oxford X-Max 50). X-ray diffraction (XRD) patterns of powder and single crystals were collected from a Bruker D8 Advance x-ray diffractometer using $\text{Cu K}\alpha$ radiation. Resistivity measurements were performed on a Quantum Design physical property measurement system (QD PPMS-14T). Magnetization mea-

^(a) These authors contributed equally to this paper.

^(b) Corresponding author. E-mail: pcheng@ruc.edu.cn

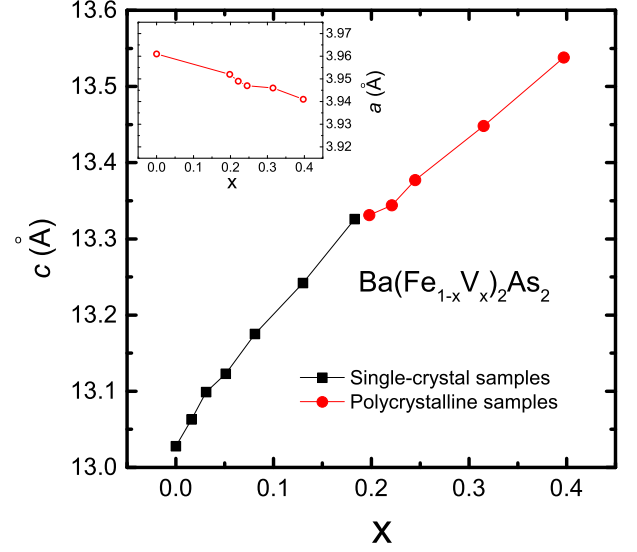
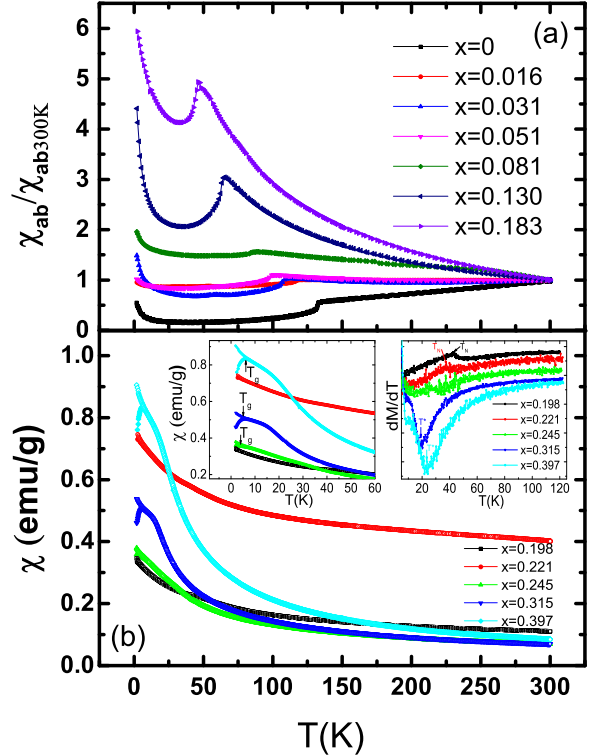
Table 1: Chemical composition analysis of $\text{Ba}(\text{Fe}_{1-x}\text{V}_x)_2\text{As}_2$.

Sample type	Nominal x	EDS x
Single crystal	0.06	0.016
Single crystal	0.1	0.031
Single crystal	0.14	0.051
Single crystal	0.20	0.081
Single crystal	0.30	0.130
Single crystal	0.40	0.183
Polycrystalline	0.26	0.198
Polycrystalline	0.29	0.221
Polycrystalline	0.30	0.245
Polycrystalline	0.40	0.315
Polycrystalline	0.50	0.397

surement was carried out in Quantum Design MPMS3. Elastic neutron scattering measurements were performed using the HB1A triple-axis spectrometer at HFIR with incident energy $E_i=14.65$ meV and collimation of $40'-40'-40'-80'$.

Results and discussion. – Single crystals with centimeter or millimeter size are obtained through self-flux crystal growth method up to nominal doping $x=40\%$. It is not possible to grow samples in single crystal form at a higher doping level. However polycrystalline samples of $\text{Ba}(\text{Fe}_{1-x}\text{V}_x)_2\text{As}_2$ with nominal doping up to $x=50\%$ can be synthesized with only a small amount of impurity phases (impurity phases including VAs are estimated to be lower than 5% from x-ray diffraction refinement). We characterized all samples with EDS and the results are listed in Table.1. Figure 1 plots the lattice parameters as a function of V concentration. The c -lattice parameter increases monotonically with increasing x which is the typical feature in hole-doped iron-pnictides material [21]. Comparing with other hole-doping cases (Mn, Cr, Mo or K) [21, 22], Vanadium substitution effectively expands the c -axis, the parameter increases 4% at $x=0.397$. On the other hand, there is a slight contraction for the a -axis lattice parameter which decreases 0.5% at $x=0.397$.

Magnetization results for $\text{Ba}(\text{Fe}_{1-x}\text{V}_x)_2\text{As}_2$ ($0 \leq x \leq 0.183$) single crystals are presented in Figure 2(a). The data were measured in zero-field-cooling (ZFC) with magnetic field of 1 T applied parallel to the ab -plane and normalized by the susceptibility at 300 K. For BaFe_2As_2 , the susceptibility decreases linearly with decreasing temperature, then drops abruptly below the AFM transition with $T_N \approx 133$ K. With V-doping, the susceptibility increases with decreasing temperature and approaches a Curie-Weiss-like behavior. The AFM transition remains sharp in all doped single crystals. Figure 2(b) shows both the ZFC and FC magnetization results for polycrystalline samples at higher doping levels ($0.198 \leq x \leq 0.397$). For $x=0.198$ and $x=0.221$, the weak AFM transitions in the magnetic susceptibility is evident from the dM/dT curves

Fig. 1: Room-temperature lattice parameters as a function of V-doping value x determined from EDS for $\text{Ba}(\text{Fe}_{1-x}\text{V}_x)_2\text{As}_2$.Fig. 2: The magnetization data for $\text{Ba}(\text{Fe}_{1-x}\text{V}_x)_2\text{As}_2$ in a field $\mu_0 H=1$ T. (a) Single crystals with $0 \leq x \leq 0.183$ measured along the ab -crystal direction. (b) Polycrystalline samples with $0.198 \leq x \leq 0.397$. The solid symbols represent the ZFC curve and the open symbols represent the FC curve. The left inset is enlarged view for $T < 60$ K and the right inset shows the temperature dependence of dM/dT .

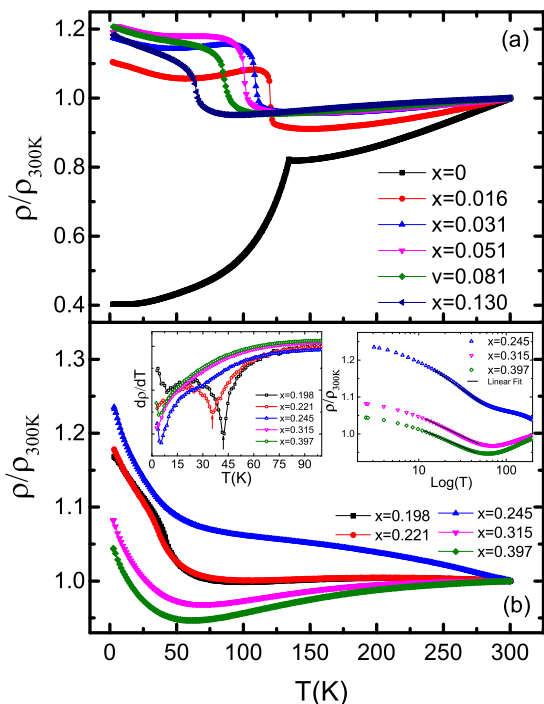


Fig. 3: Temperature dependence of electrical resistivity for $\text{Ba}(\text{Fe}_{1-x}\text{V}_x)_2\text{As}_2$. (a) Single crystal data with $0 \leq x \leq 0.13$ measured along the ab direction. (b) Polycrystalline data with $0.198 \leq x \leq 0.397$. Left inset shows the T -dependence of $d\rho/dT$ and right inset shows the $\log(T)$ -dependence of resistivity.

with $T_N \approx 43$ K and 37 K respectively (inset of Figure 2(b)). For $x=0.245$, No sign of magnetic transition can be inferred from the M - T curve, while the separation between ZFC and FC susceptibilities at low temperatures indicates a spin glass behavior (SG). Such behavior becomes even more apparent for $x=0.315$ and $x=0.397$ samples. Furthermore, for $x=0.315$ and $x=0.397$ there are new AFM-like kinks (marked as T^*) in the M - T curves at around 20 K, indicating possible new short-range AFM fluctuations. In addition, we calculated the paramagnetic moments from the Curie-Weiss fit of susceptibility data for heavily V-doped samples ($x=0.315$ and $x=0.397$). Assuming all the moment contribution is from V, the results show that the average moment brought by one V ion is about $2.9\mu_B$, which is quite close to the theoretical moment value of one free V^{3+} ion.

Figure 3 presents the normalized electrical transport data ρ/ρ_{300K} . The temperature dependent resistivity for BaFe_2As_2 shows a sharp drop anomaly at the AFM/structural transition, while for the V-doped samples the feature becomes a sharp upturn and gradually moves to lower temperatures with increasing x . The temperatures of resistivity anomalies determined from the minimum of $d\rho/dT$ are consistent with the T_N from the M - T curves. At $x=0.198$ and $x=0.221$, the weak features

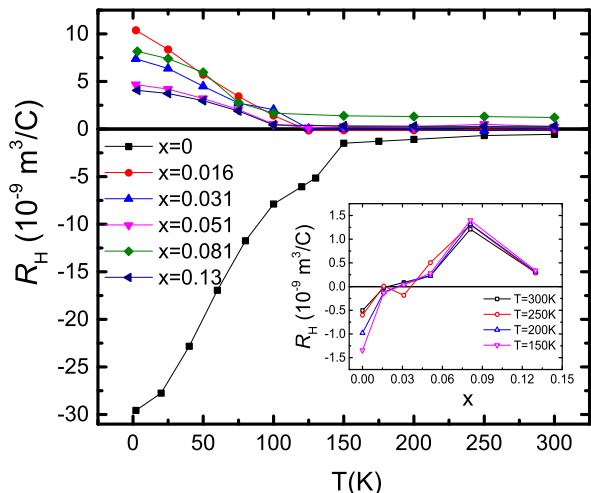


Fig. 4: The temperature dependence of Hall coefficient R_H for $\text{Ba}(\text{Fe}_{1-x}\text{V}_x)_2\text{As}_2$ ($0 \leq x \leq 0.13$). The inset shows doping dependence of R_H at different temperatures.

of resistivity anomalies are still visible from the $d\rho/dT$ curves as shown in the inset of Figure 3(b). However from $x \geq 0.245$, such anomaly could not be detected anymore, indicating the absence of AFM/structural transition. Furthermore, the resistivity increases approximately logarithmically with decreasing temperature below 50 K as shown in the right inset of Figure 3(b), which is a characteristic of Kondo scattering. This behavior suggests that the Vanadium dopants act as magnetic impurities.

The Hall coefficients R_H at different temperatures for $\text{Ba}(\text{Fe}_{1-x}\text{V}_x)_2\text{As}_2$ ($0 \leq x \leq 0.13$) single crystals are presented in figure 4. R_H changes suddenly from a negative value in the undoped sample to a positive one with slight V-doping at low temperatures, and becomes completely positive in all temperature region measured at $x=0.051$. Comparing to the Hall effect in Cr-doping [5], the sign-reversal of R_H occurs at a much lower doping level indicates that V acts as an effective hole dopant. The doping dependence of R_H at different temperatures is shown in the inset of Figure 4. After changing sign ($x > 0.04$), The value of $R_H(T)$ initially increases then decreases at $x=0.130$. This feature is quite similar to the Hall effect in $\text{Ba}_{0.6}\text{K}_{0.4}\text{Fe}_2\text{As}_2$ [23], which is explained as the result of asymmetric scattering between the electron and hole bands where the mobility is much larger for the former [20, 23].

Neutron diffraction experiments were performed on single crystals at $x=0.031$, 0.051 and 0.130 , the results are shown in figure 5(a)-(c). The AFM transition was characterized by measuring the temperature dependence of $(0.5 \ 0.5 \ 1)_T$ magnetic Bragg peak and the tetragonal to orthorhombic structural transition is identified by the intensity change of the $(1 \ 1 \ 2)_T$ nuclear peak (T refers to tetragonal basis) [24]. Combing the neutron scattering data and resistivity results of $d\rho/dT$, where only one tran-

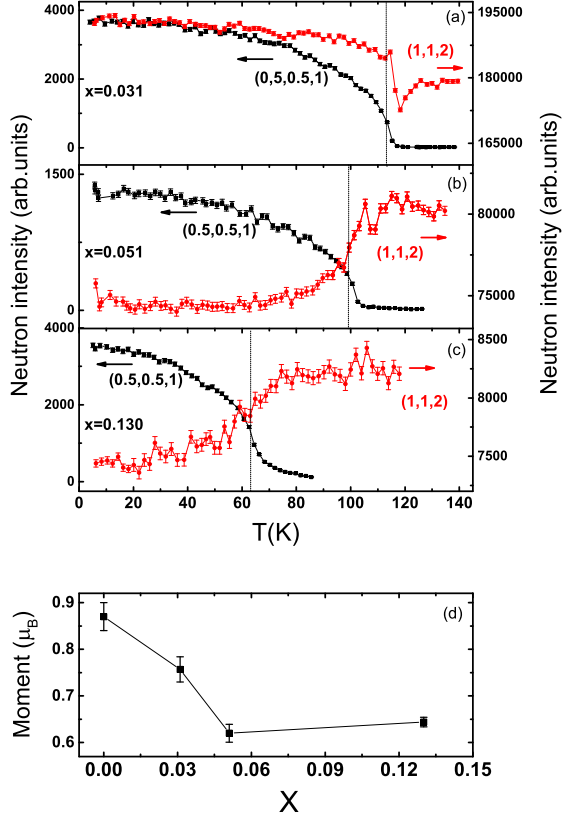


Fig. 5: Neutron diffraction results for the $x=0.031$ (a), $x=0.051$ (b) and $x=0.130$ (c) single crystals. The temperature dependence of magnetic Bragg peak $(0.5\ 0.5\ 1)_T$ is shown in black squares and that of nuclear Bragg peak $(1\ 1\ 2)_T$ is shown in red circles. (d) Refined magnetic moments for $x = 0, 0.031, 0.051, 0.130$ at $T=5$ K. The refinements were carried out using Fullprof software based on the neutron diffraction data.

sition anomaly is observed, both the structural and magnetic transitions occur at the same temperature for V-doped samples. This agrees with other hole-doped FeAs-122 cases (Cr, Mn, Mo and K) [6, 7, 19, 25], but different from the electron-doping cases in which T_S and T_N are well separated [26]. The doping dependence of the refined magnetic moment is presented in figure 5(d). For the electron-doping cases such as Co-doped BaFe_2As_2 , the ordered moment is linearly suppressed with doping and finally becomes zero with 5% Co-doping [27]. For the hole-doping cases like $\text{Ba}(\text{Fe}_{1-x}\text{Cr}_x)_2\text{As}_2$, the magnetic moment is independent of concentration for $x \leq 0.2$ despite suppression of the transition temperature from 133 K to 56 K. Then the moment quickly decreases to about $0.3\mu_B$ at $x=0.335$ [6]. While for V-doping case, the moment evolution seems to be slightly different. The average ordered Fe/V moment first decreases in the range of $0 \leq x \leq 0.051$, then becomes almost doping independence from $x=0.051$

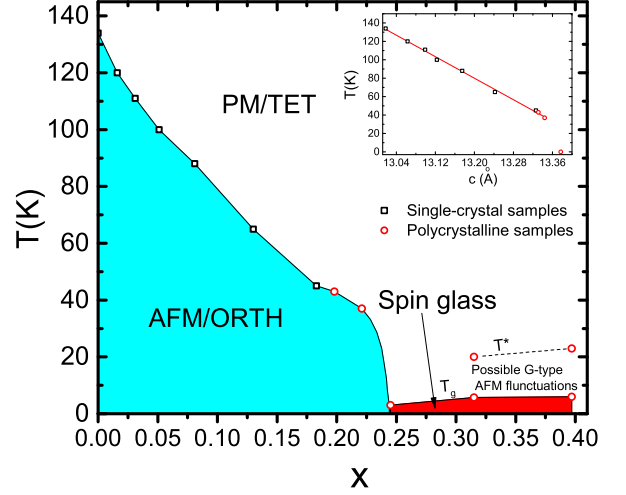


Fig. 6: Compositional-Temperature phase diagram for $\text{Ba}(\text{Fe}_{1-x}\text{V}_x)_2\text{As}_2$. Spin glass temperature T_g and possible G-type AFM fluctuation temperature T^* are defined in figure 2. The AFM transition temperature versus c lattice parameter plot is shown in the inset. The linear fitting result is shown as the red solid line.

($0.62\mu_B$) to $x=0.13$ ($0.64\mu_B$).

Based on the experimental results above, the T - x phase diagram for V-doped BaFe_2As_2 is presented in figure 6. There is a gradual suppression of the AFM/structural transition temperature of BaFe_2As_2 from 133 K to 37 K with increasing x . The decreasing of AFM transition temperature actually follows a linear behavior with increasing c , see the inset of figure 6. Usually one would expect an doping-induced magnetic quantum critical point. However the AFM/structural transition suddenly vanishes at $x=0.245$ and $c=13.54\text{\AA}$. On the other hand, a spin glass state is detected on the vanishing point of AFM order. These observations strongly suggest an avoided quantum critical point (QCP) by the development of competing states [26, 28]. Magnetic QCP should not be a necessary condition for Fe-based superconductivity, it is interesting to mention that for Co- or Ni-doped BaFe_2As_2 , near the optimal doping with maximum T_c , there were also reports about an avoided QCP [26] and clustered spin glass state [10, 11]. The spin glass in $\text{BaFe}_{2-x}(\text{Co/Ni})_x\text{As}_2$ was previously interpreted as an intrinsic response to the competition between the superconductivity and antiferromagnetism [10], but similar explanation is not applicable for the SG in $\text{Ba}(\text{Fe}_{1-x}\text{V}_x)_2\text{As}_2$ since no superconductivity was observed for the V-doped samples. The most plausible explanation is that the magnetic impurity V in metallic hosts could result in the Ruderman-Kittel-Kasuya-Yosida (RKKY) effective exchange interaction between the impurity spins, which leads to a spin glass behavior [29, 30].

The AFM-like kinks (T^*) observed in M-T curves at $x=0.315, 0.397$ closely resemble the behavior of checkerboard (G-type) AFM order in Cr- and Mn-doped

BaFe₂As₂ [6, 7]. According to calculations in Mn-doped BaFe₂As₂, the doped magnetic impurities would exhibit a G-type magnetic structure close to their cores in heavily doped region when the RKKY interactions between the conducting electrons and the magnetic impurities are taken into account [29]. Similarly, the T* in the V-doped samples most probably represents the formation of short-range local G-type AFM fluctuations. The Fe-based superconductivity may be accompanied by the spin fluctuations of the 3d electrons of Fe which are possibly suppressed by the competition of G-type spin fluctuations brought by V.

Conclusion. – As a magnetic impurity, the doping of V into BaFe₂As₂ suppresses the AFM order and generate effective hole-doping effect, no superconductivity is observed which is in contrast with the K-doped BaFe₂As₂. This indicates the extreme sensitivity of in-plane magnetic impurity for Fe-based superconductivity. On the other hand, the RKKY spin glass behavior accompanied by possible checkerboard antiferromagnetic fluctuations emerges at higher doping levels. The phase diagram of Ba(Fe_{1-x}V_x)₂As₂ exhibits an avoided QCP similar as that in Ni-doped BaFe₂As₂.

The work at RUC is supported by NSFC (No.11204373 and No.11227906).

REFERENCES

- [1] LEE PATRICK A., NAGAOSA NAOTO, and WEN XIAO-GANG, *Rev. Mod. Phys.*, **78** (2006) 17.
- [2] HOSONO HIDEO, TANABE KEIICHI, TAKAYAMA-MUROMACHI EIJI, KAGEYAMA HIROSHI, YAMANAKA SHOJI, KUMAKURA HIROSHI, NAHARA MINORU, HIRAMATSU HIDENORI, and FUJITSU SATORU, *Sci. Technol. Adv. Mater.*, **16** (2015) 033503.
- [3] BAO WEI, *Chin. Phys. B*, **22** (2013) 087405.
- [4] LUO HUIQIAN, ZHANG RUI, LAVER MARK, YAMANI ZAHRA, WANG MENG, LU XINGYE, WANG MIAOYIN, CHEN YANCHAO, LI SHILIANG, CHANG SUNG, LYNN JEFFREY W., and DAI PENGCHENG, *Phys. Rev. Lett.*, **108** (2012) 247002.
- [5] SEFAT ATHENA S., SINGH DAVID J., VANBEBBER LINDSAY H., MOZHARIVSKYJ YURIJ, MCGUIRE MICHAEL A., JIN RONGYING, SALES BRIAN C., KEPPENS VEERLE, and MANDRUS DAVID, *Phys. Rev. B*, **79** (2009) 224524.
- [6] MARTY K., CHRISTIANSON ANDREW D., WANG C. H., MATSUDA M., CAO H., VANBEBBER L. H., ZARESTKY J. L., SINGH DAVID J., SEFAT ATHENA S., and LUMSDEN MARK D., *Phys. Rev. B*, **83** (2011) 060509(R).
- [7] KIM M. G., KREYSSIG A., THALER A., PRATT D. K., TIAN W., ZARESTKY J. L., GREEN M. A., BUD'KO S. L., CANFIELD P. C., MCQUEENEY R. J., and GOLDMAN A. I., *Phys. Rev. B*, **82** (2010) 220503(R).
- [8] ZHOU R., LI Z., YANG J., SUN D. L., LIN C. T., and ZHENG G. Q., *Nat. Commun.*, **4** (2013) 2265.
- [9] ALLRED J. M., TADDEI K. M., BUGARIS D. E., KROGSTAD M. J., LAPIDUS S. H., CHUNG D. Y., CLAUS H., KANATZIDIS M. G., BROWN D. E., KANG J., FERNANDES R. M., EREMIN I., ROSENKRANZ S., CHMAISSEM O., and OSBORN R., *Nat. Phys.*, **12** (2016) 493.
- [10] DIOGUARDI A. P., CROCKER J., SHOCKLEY A. C., LIN C. H., SHIRER K. R., NISSON D. M., LAWSON M. M., APROBERTS-WARREN N., CANFIELD P. C., BUD'KO S. L., RAN S., and CURRO N. J., *Phys. Rev. Lett.*, **111** (2013) 207201.
- [11] LU XINGYE, TAM DAVID W., ZHANG CHENGLIN, LUO HUIQIAN, WANG MENG, ZHANG RUI, HARRIGER LELAND W., KELLER T., KEIMER B., REGNAULT L.-P., MAIER THOMAS A., and DAI PENGCHENG, *Phys. Rev. B*, **90** (2014) 024509.
- [12] SEFAT ATHENA S., JIN RONGYING, MCGUIRE MICHAEL A., SALES BRIAN C., SINGH DAVID J., and MANDRUS DAVID, *Phys. Rev. Lett.*, **101** (2008) 117004.
- [13] NI N., THALER A., YAN J. Q., KRACHER A., COLOMBIER E., BUD'KO S. L., CANFIELD P. C., and HANNAHS S. T., *Phys. Rev. B*, **82** (2010) 024519.
- [14] HAN FEI, ZHU XIYU, CHENG PENG, MU GANG, JIA YING, FANG LEI, WANG YONGLEI, LUO HUIQIAN, ZENG BIN, SHEN BING, SHAN LEI, REN CONG, and WEN HAI-HU, *Phys. Rev. B*, **80** (2009) 024506.
- [15] ZHU XIYU, HAN FEI, MU GANG, TANG JUN, JU JING, TANIGAKI KATSUMI, WEN HAI-HU, *Phys. Rev. B*, **81** (2010) 104525.
- [16] SHARMA SHILPAM, BHARATHI A., CHANDRA SHARAT, REDDY RAGHAVENDRA, PAULRAJ S., SATYA A. T., SAS-TRY V. S., GUPTA AJAY, SUNDAR C. S., *Phys. Rev. B*, **81** (2010) 174512.
- [17] JIANG SHUAI, XING HUI, XUAN GUOFANG, WANG CAO, REN ZHI, FENG CHUNMU, DAI JIANHUI, XU ZHU-AN and CAO GUANGHAN, *J. Phys.: Condens. Matter*, **21** (2009) 382203.
- [18] ROTTER MARIANNE, TEGEL MARCUS, JOHRENDT DIRK, *Phys. Rev. Lett.*, **101** (2008) 107006.
- [19] SEFAT ATHENA S., MARTY KAROL, CHRISTIANSON ANDREW D., SAPAROV BAYRAMMURAD, MCGUIRE MICHAEL A., LUMSDEN MARK D., TIAN WEI, and SALES BRIAN C., *Phys. Rev. B*, **85** (2012) 024503.
- [20] ZHANG LEI, LUO HUIQIAN, CHENG PENG, WANG ZHAOSHENG, JIA YING, MU GANG, SHEN BING, MAZIN I. I., SHAN LEI, REN CONG, and WEN HAI-HU, *Phys. Rev. B*, **80** (2009) 140508(R).
- [21] KONZEN LANCE M.N., and SEFAT ATHENA S., *J. Phys.: Condens. Matter*, **29** (2017) 083001.
- [22] ROTTER MARIANNE, PANGERL MICHAEL, TEGEL MARCUS, and JOHRENDT DIRK, *Angew. Chem. Int. Ed.*, **47** (2008) 7949.
- [23] SHEN BING, YANG HUAN, WANG ZHAO-SHENG, HAN FEI, ZENG BIN, SHAN LEI, REN CONG, and WEN HAI-HU, *Phys. Rev. B*, **84** (2011) 184512.
- [24] HUANG Q., QIU Y., BAO WEI, GREEN M. A., LYNN J. W., GASPAROVIC Y. C., WU T., WU G., and X. H. CHEN, *Phys. Rev. Lett.*, **101** (2008) 257003.
- [25] CHEN H., REN Y., QIU Y., BAO WEI, LIU R. H., WU G., WU T., XIE Y. L., WANG X. F., HUANG Q., and CHEN X. H., *Europhys. Lett.*, **85** (2009) 17006.
- [26] LU XINGYE, GRETARSSON H., ZHANG RUI, LIU XUERONG, LUO HUIQIAN, TIAN WEI, LAVER MARK, YA-

- MANI Z., KIM YOUNG-JUNE, NEVIDOMSKYY A. H., SI QIMIAO, and DAI PENGCHENG, *Phys. Rev. Lett.*, **110** (2013) 257001.
- [27] LESTER C., CHU JIUN-HAW, ANALYTIS J. G., CAPELLI S. C., ERICKSON A. S., CONDRON C. L., TONEY M. F., FISHER I. R., and HAYDEN S. M., *Phys. Rev. B*, **79** (2009) 144523.
- [28] GOKO TATSUO, ARGUELLO CARLOS J., HAMANN ANDREAS, WOLF THOMAS, LEE MINHYEA, REZNIK DMITRY, MAISURADZE ALEXANDER, KHASANOV RUSTEM, MORENZONI ELVEZIO, and UEMURA YASUTOMO J., *npj Quantum Materials*, **2** (2017) 44.
- [29] GASTIASORO MARIA N. and ANDERSEN BRIAN M., *Phys. Rev. Lett.*, **113** (2014) 067002.
- [30] BINDER K. and YOUNG A. P., *Rev. Mod. Phys.*, **58** (1986) 801.